A R C H I V E S O F M E T A L L U R G Y A N D M A T E R I A L S
Volume 51 2006 Issue 2

E. KAWECKA-CEBULA*, Z. KALICKA*, J. WYPARTOWICZ*

FILTRATION OF NONMETALLIC INCLUSIONS IN STEEL

FILTRACJA WTRĄCEŃ NIEMETALICZNYCH W STALI

A model of the adhesion between two inclusion particles in liquid metal, which corresponds to metal filtration by means of ceramic filters, have been developed. The adhesion originates from gas neck formation in the region of particles contact due to the poor wetting between metal and inclusions. The neck radius is the main geometric parameter of the model, which correlates the collision efficiency coefficient with the adhesion force. The method of calculation of the neck radius from particles dimensions and surface energies in the system was elaborated, and the dependence between adhesion force and collision efficiency coefficient was proposed. The experimental data from literature were used to check the model by calculation the adhesion force for various combinations of inclusions sizes. This force is of the order 10^{-5} N for particles bigger than 10^{-6} m and it grows with particle size. The results of calculations show, that attraction is stronger if one particle is much larger than another. This means, that interaction of particle is stronger with filter wall, than with another particle.

Keywords: nonmetallic inclusions, liquid steel, filtration, adhesion, wetting angle

Opracowano model adhezji między dwoma cząstkami wtrąceń niemetalicznych w ciekłym metalu, co odpowiada filtracji metalu z użyciem filtrów ceramicznych. Przyczyną adhezji jest powstanie szyjki wypełnionej gazem w miejscu kontaktu wtrąceń, co jest spowodowane słabą zwilżalnością między metalem a wtrąceniami. Promień szyjki jest głównym parametrem geometrycznym modelu, który wiąże współczynnik skuteczności zderzeń z siłą adhezji. Opracowano metodę obliczania promienia szyjki na podstawie promieni cząstek i energii międzyfazowych w układzie oraz zaproponowano zależność między siłą adhezji a współczynnikiem skuteczności zderzeń. Na podstawie danych doświadczalnych z literatury dokonano weryfikacji modelu poprzez obliczenie siły adhezji dla różnych kombinacji rozmiarów cząstek. Siła ta jest rzędu 10^{-5} N dla cząstek większych niż 10^{-6} m i rośnie wraz ze wzrostem rozmiarów cząstek. Wyniki obliczeń wskazują, że siła adhezji jest większa, gdy jedna z cząstek jest znacznie większa, niż druga. Oznacza to, że oddziaływanie cząstki ze ścianą filtra jest silniejsze, niż z drugą cząstką o podobnych rozmiarach.

1. Introduction

Liquid steel filtration is the operation promising from the view-point of attaining high steel purity. This is of special importance in the grades assigned for deep drawing, where bigger inclusions, mainly alumina based ones, make the process impossible. To implement this operation into common industrial practice more knowledge has to be gained on filtration mechanism and filters operation. Present work analyses the basic physical interaction in filtration process, i.e. attraction between two inclusion particles. This analysis may be also adopted to interaction of particle with filter wall. More complex case of simultaneous interaction of particle with two or more others is not considered in the present work.

2. Model of filtration

In the process of retaining the inclusions in the filter interior, three stages can be distinguished:

- Transport of inclusion from the bulk of metal to the surface of filter pores,
- Adhesion of inclusions at the filter surface,
- Durable bonding as a result of sintering with filter material.

The first stage is decisive for the efficiency of filtration. Transport of inclusions may occur through diffusion or convection with the stream of flowing steel. Due to small pores diameter as well as to the limited flow rate of steel stream, the flow in filter pores is laminar [4, 5]. In such conditions, where the residence time of

* FACULTY OF METALS ENGINEERING AND INDUSTRIAL COMPUTER SCIENCE, AGH UNIVERSITY OF SCIENCE AND TECHNOLOGY, 30-059 KRAKÓW, 30 MICKIEWICZA AVE., POLAND

steel in the pore is short, the diffusive transport from the centre of the stream to the walls of the channel is meaningless. This opinion was confirmed experimentally by Uemura *et al.* [1], who compared the calculation by means of diffusion model with measured efficiencies for loop filter. The calculated efficiencies were several times lower than these from the experiment. The collisions of inclusions with filter surface and their retaining takes place predominantly at the filter entry, where stirring is strong due to the abrupt change of flow direction and fragmentation of stream. In farther regions of filter only the inclusions traveling in the nearest vicinity of filter walls may be attached and retained. Thus the amount of adhering inclusions falls strongly with increasing distance from filter entry.

The inclusions in steel subjected to filtration come mainly from deep deoxidization, usually with the use of aluminum. The filtration efficiency may be expressed through the change in inclusions number or the change in the concentration of insoluble oxygen bonded in oxide form. The number of inclusions might be the reliable criterion in the case of uniform particle size. The filter captures mainly large inclusions, while small ones, which are abundant, are difficult to catch. The most unfavorable for steel quality are large inclusions (~ 80 μm) and high total oxygen level. The limited amount of very fine inclusions is even beneficial for steel quality. That is why the filtration efficiency may be expressed in terms of the decrease in quantity of oxide inclusions, which is equivalent to decrease of insoluble oxygen concentration, or insoluble aluminum concentration, as the inclusions consist mainly of Al_2O_3. If the inclusions consist only of oxides, the rate of inclusions capture from the metal flowing through filter pores may be described as [1]:

$$-\frac{d[\%O_{ins}]}{dt} = \frac{(A_f dx)S}{(A_f dx)\varepsilon} \cdot [\%O_{ins}] \cdot \beta \cdot v, \qquad (1)$$

where:

$[\%O_{ins}]$ – content of oxygen bonded in inclusions,

A_f – area of transverse section of the filter,

S – active surface index of the filter,

x – filter length,

ε – porosity of the filter,

β – coefficient of effective collisions of inclusions with filter,

v – linear velocity of flow of liquid metal through the filter.

Active surface index S of the filter denotes the area of internal filtering surface and it refers to filter unit volume. The velocity of flow of liquid metal inside the filter is expressed as:

$$v = \frac{dx}{dt} \qquad (2)$$

The filtration efficiency η is defined as:

$$\eta = \frac{[\%O_{ins}]^0 - [\%O_{ins}]}{[\%O_{ins}]^0}, \qquad (3)$$

where the upper index "0" refers to the initial state prior to filtration.

In liquid steel filtration various types of filters are applied, as: loop, monolithic, foam and layer type. In the present work two main types are considered: loop and monolithic, which are schematically presented in Fig. 1. Loop filter is made of a scrolls of ceramic thread, usually 2÷5 mm in diameter. In the monolithic (or multi-hole) filter metal flows through parallel channels. In the case of loop filters the active surface S may be determined as [1]:

$$S = \frac{d_f l}{(\pi d_f^2 l)/(4(1-\varepsilon))} = \frac{4(1-\varepsilon)}{\pi d_f}. \qquad (4)$$

The loop filters are characterized with two parameters:

l – the thread length within the specified filter volume, and

d_f – the thread diameter.

From combination of equations (1), (3) and (4) the filtration efficiency may be determined:

$$\ln(1-\eta) = -\frac{4(1-\varepsilon)}{\pi d_f \varepsilon} \cdot \beta \cdot L. \qquad (5)$$

where L – the filter length.

The channels in the monolithic filters have the square or circular cross section, which is characterized by the side a or diameter d, respectively. The active surface of such filter, respective to the shape of channels, is given as:

$$S = \frac{4\varepsilon}{d} \quad or \quad S = \frac{4\varepsilon}{a} \qquad (6)$$

From equations (1), (3) and (6) the efficiency of monolithic filters may be determined as:

$$\ln(1-\eta) = -\frac{4}{d} \cdot \beta \cdot L \quad or \quad \ln(1-\eta) = -\frac{4}{a} \cdot \beta \cdot L. \qquad (7)$$

One must take into account, that some of the inclusions, which got in contact with filter walls do not form stable connection. This effect is expressed in coefficient of collision efficiency β.

The adhesion of particle to the filter wall is the second stage of filtration. The particles adhere directly to filter material only in very early stage of filtration. Later

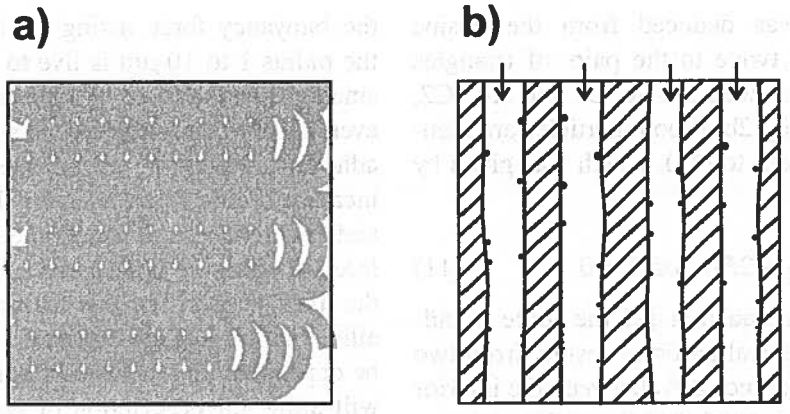

Fig. 1. Schematic diagram of two types of filters considered in the present work: a) loop filter (metal flow perpendicular to the figure surface), b) monolithic filter

on particles adhere to inclusions which were previously fixed and sintered with filter walls.

In the present work simplified model of adhesion was adopted:

- It is assumed that the filtration efficiency is dependent on the behavior of single inclusions.
- Only small fraction of particles is detained directly on filter material. The majority sticks to the particles already detained.
- Two cases of the adhesion of two spherical particles are considered:
  1) Equal radii r, what corresponds to the interaction of two inclusions,
  2) Various radii r_1 and r_2, what corresponds to interaction between two inclusions or between the inclusion and the filter wall.
- The contact angle Θ in the system inclusion – liquid metal – gas is the main factor determining particle-wall and particle-particle interactions.
- The detaching forces – buoyancy and drag resulting from viscous metal flow are small in comparison to adhesive forces. These forces may be effective in the case of inclusions, which are better wetted by metal, eg. SiO_2 and MgO [1,8] or at very high velocities of flow.

If two spherical particles of radii r_1 and r_2, which are poorly wetted by steel, approach, the steel in contact area withdraws, leaving the empty (filled with gases and vapors) neck of concave lens shape. This is schematically illustrated in Fig. 2a. The present authors recommend the method of calculation the neck dimensions with the use of auxiliary variable R_2'. The radius of the neck R_2 may be calculated from the relations:

$$(r_1 + r_2)\left(R_2'^2 + 2R_1R_2'\right) + 2r_1r_2R_1\left(\cos\Theta_1 + \cos\Theta_2\right) = 0 \tag{8}$$

$$R_2' = R_2/\sin\alpha = R_2/\sqrt{1-\cos^2\alpha} \tag{9}$$

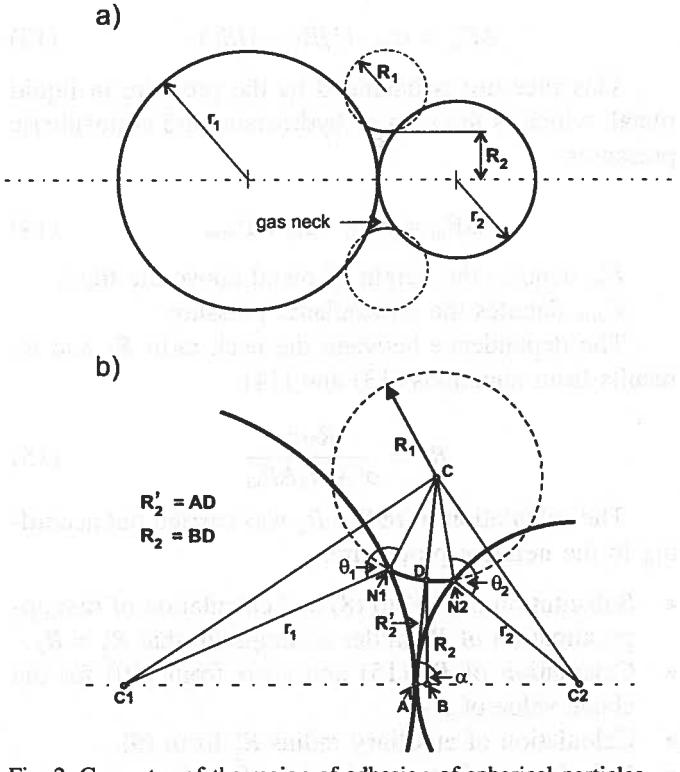

Fig. 2. Geometry of the region of adhesion of spherical particles

$$\cos\alpha = \frac{R_1\left(r_1\cos\Theta_1 - r_2\cos\Theta_2\right)}{(r_1+r_2)\left(R_1+R_2'\right)} \tag{10}$$

R_1 denotes the curvature radius of metal surface in the neck region

R_2' – auxiliary variable ($R_2' = R_2$ if $r_1 = r_2$).

Θ_1, Θ_2 – wetting angles between particles material and liquid steel,

α – the angle between R_2' and the straight line connecting the centers of particles.

The relation (8) was deduced from the cosine law, which was applied twice to the pairs of triangles C-C1-N1 and C-C2-N2 as well as A-C-C1 and A-C-C2, which are presented in Fig. 2b. If both particles are identical, equation (10) reduces to (11), which was given by Sasai *et al.* [2].

$$R_2^2 + 2R_1R_2 + 2R_1 r\cos\Theta = 0. \tag{11}$$

According to Fisher equation [2] the force of adhesion between two spherical particles results from two sources: the pressure difference ΔP_m between the interior of the neck and the liquid metal, and the surface tension of metal σ_m.

$$F_{adh} = \pi \cdot R_2^2 \cdot \Delta P_m + 2\pi \cdot R_2 \cdot \sigma_m. \tag{12}$$

The difference in pressure ΔP_m, termed the bubble pressure is expressed by the Laplace equation:

$$\Delta P_m = \sigma_m \cdot (1/R_1 - 1/R_2). \tag{13}$$

This pressure is balanced by the pressure in liquid metal, which is the sum of hydrostatic and atmospheric pressures:

$$\Delta P_m = \rho \cdot g \cdot H_m + P_{atm} \tag{14}$$

H_m denotes the height of metal above the filter,
P_{atm} denotes the atmospheric pressure.

The dependence between the neck radii R_1 and R_2 results from equations (13) and (14):

$$R_1 = \frac{R_2\sigma}{\sigma + R_2\Delta P_m} \tag{15}$$

The calculation of radius R_2 was carried out according to the iterative procedure:

- Substitution of (15) to (8) and calculation of first approximation of R_2 under assumption, that $R_2' = R_2$.
- Calculation of R_1 (15) and cosα from (10) for the above value of R_2.
- Calculation of auxiliary radius R_2' from (9).
- Calculation of corrected value of R_2 from (8).
- Renewed calculation of R_1, cosα and R_2'.
- Renewed calculation of R_2 etc.

The above procedure is quickly convergent.

3. Dependence between force of adhesion and efficiency of collisions

In the third stage of filtration the inclusions should be firmly bonded with filter material through sintering, provided that they were not washed off by the drag force of metal flow or buoyancy. Sasai *et al.* [2] estimated that the buoyancy force acting on the spherical particle of the radius 1 to 10 μm is five to six orders of magnitude smaller than the force of adhesion. The drag force, however, is only one to three orders smaller than the force of adhesion, depending on the metal stream velocity. The increase of this velocity favors the severance of particles and thus reduces the filtration efficiency. That is why the force of adhesion is decisive in retaining the particles at the filter surface. For this reason the coefficient β of the efficiency of particle collisions with filter walls should be dependent on the force of adhesion. This dependence will allow for description of two stages of filtration by means of common model, basing on most important process parameters.

The authors of the present work suggest the linear relation:

$$\beta = a + b \cdot F_{adh}. \tag{16}$$

The available experimental data allow only to use this simplest dependence.

In order to determine the coefficients a and b in equation (16) the experimental data from the literature were employed for loop filters [1, 3] and for monolithic filters [3, 4]. These used in the calculations are collected in Table 1.

For the calculations the coefficient β the data on surface tension σ, density ρ as well as the composition and temperature of the metal filtered are also necessary. The data on surface tension of liquid iron at its melting temperature differ within the range 1.6 to 1.9 N/m. Even small amount of surface active elements, as oxygen and sulphur, strongly influences the surface tension. In the present work the following dependence was employed [8]:

$$\begin{aligned}\sigma_{Fe} = {} & 1.87 - 1.05 \cdot \%[S] - 0.95 \cdot \%[O] - 0.1 \cdot \%[N] \\ & - 0.01 \cdot \%[C] - 0.01 \cdot \%[Si] \\ & - 0.00049 \cdot \left(T - T_{liq}\right)[N/m]\end{aligned} \tag{17}$$

$$\begin{aligned}T_{liq} = {} & 1812 - 65 \cdot \%[C] - 8 \cdot \%[Si] - 5 \cdot \%[Mn] \\ & - 25 \cdot \%[S] - 80 \cdot \%[O][K],\end{aligned} \tag{18}$$

where T_{liq} denotes the liquidus temperature of steel.

The wetting angle between Al_2O_3 and liquid steel is also dependent on the concentration of oxygen and sulphur in steel. The concentration of sulphur does not considerably change during filtration, while the variation of oxygen content may be more distinct. In the present work this influence is estimated as:

$$\Theta_{Al_2O_3-Fe} = 132 - 788.5 \cdot \%\ [O] \tag{19}$$

TABLE

Parameters of filtration experiments employed in the determination of coefficients of equation (11)

Loop filters, $\varepsilon = 0.63$											
Ref	η	d_f, [mm]	L, [mm]	v, [cm/s]	[O], [%]	r mean [μm]	r min, [μm]	r max, [μm]	H_m, [m]	T, [K]	Steel comp., [%]
[1]	0.87	2	40	2	0.005	2.5	2	3	0.07	1850	0.35C; 0.25Si
	0.84	2	40	÷	0.005	5	4.5	5.5	0.07	1850	0.75Mn
	0.99	2	40	10	0.005	10	9	11	0.07	1850	<0.03S
[3]	0.35	5	25		0.0248	1.75	1	2.5	0.5	1845	0.1C
	0.25	5	25	10	0.0248	3.75	2.55	5	0.5	1845	0.25Si
	0.5	5	25		0.0248	7.5	5.05	10	0.5	1845	0.05Al
	0.407	3	25		0.0049	1.75	1	2.5	0.5	1845	<0.03S
	0.5	3	25	7.6	0.0049	3.75	2.55	5	0.5	1845	
	0.8	3	25		0.0049	7.5	5.05	10	0.5	1845	
	0.77	2	25		0.0228	1.75	1	2.5	0.5	1845	
	0.83	2	25	5.5	0.0228	3.75	2.55	5	0.5	1845	
	0.875	2	25		0.0228	7.5	5.05	10	0.5	1845	
Monolithic filters											
Ref	η	d_f, [mm]	L, [mm]	v, [cm/s]	[O], [%]	r mean [μm]	r min, [μm]	r max, [μm]	H_m, [m]	T, [K]	Steel comp., [%]
[4]	0.879	0.74	50		0.002	0.125	0.01	0.25	0.07	1873	0.012C;
	0.97	0.74	50	0.08		0.375	0.255	0.5	0.07	1873	0.04Ni
	0.988	0.74	50			0.625	0.505	0.75	0.07	1873	
	0.711	0.74	50			0.125	0.01	0.25	0.07	1873	
	0.43	0.74	50			0.375	0.255	0.5	0.07	1873	
	0.642	0.74	50	0.15		0.625	0.505	0.75	0.07	1873	
	0.79	0.74	50			0.875	0.755	1	0.07	1873	
	0.88	0.74	50			1.125	1.05	1.25	0.07	1873	
	0.918	0.74	100			0.125	0.01	0.25	0.07	1873	
	0.951	0.74	100	0.13		0.375	0.255	0.5	0.07	1873	
	0.942	0.74	100			0.625	0.505	0.75	0.07	1873	
[3]	0.77	2.1	22.5	9	0.0197	15	7.5	20	0.5	1845	pure iron
	0.79	2.1	22.5	9	0.0159	15	7.5	20	0.5	1845	
	0.9*	1.5	22.5	2	0.0242	15	7.5	20	0.5	1845	

* – filter clogging

This relation was obtained as a linear combination of the values of contact angle of pure iron – 132° and the value 90° for oxygen concentration 0.052%, quoted by [2]. The density of liquid steel was assumed as 7000 kg/m^3.

4. Results of calculations

The results of calculations for loop filters are presented in Fig. 3, while these for monolithic filters in Figs. 4 and 5. Figs. 4 and 5 show the dependence of collision efficiency coefficient β on the force of adhesion F_{adh}, which was calculated according to two chosen variants for monolithic filters for various velocities of metal flow through the filter. Fig. 4 regards the case of particles of equal size, which corresponds to the middle of size range. Fig. 5 regards the case of particles of different sizes, which correspond to the limiting values of size range (r_1 – lower limit, r_2 – upper limit).

It may be concluded from the above results, that experimental data from different sources for loop filters [1, 3] and monolithic filters [3, 4] confirm the postulated dependence of collision efficiency coefficient on the force of adhesion. The obtained dependences are as follows:

- For loop filters and the particles of equal sizes (Fig. 3):

$\beta = 0.083 + 4644 \cdot F_{adh}$ with correlation coefficient $R^2 = 0.57$

• For loop filters and the particles of various sizes (Fig. 3):

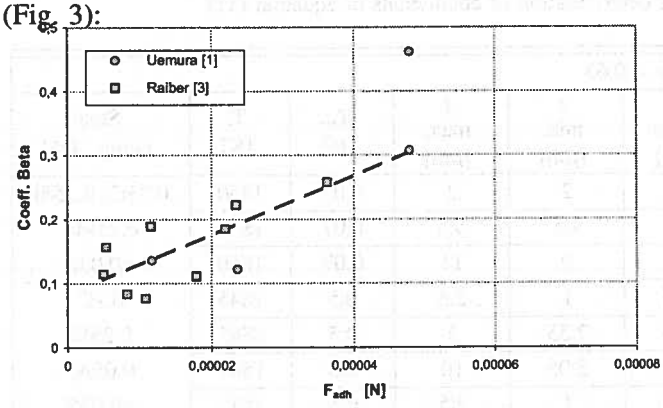

Fig. 3. Dependence of the coefficient of filtration efficiency β on the force of adhesion F_{adh} for the loop filter. The particles are of equal size.

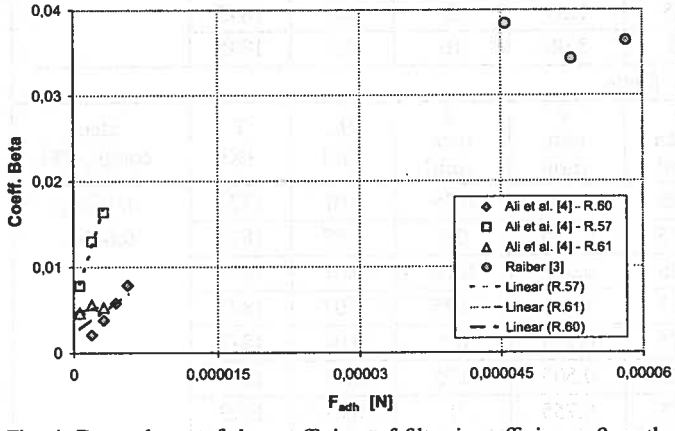

Fig. 4. Dependence of the coefficient of filtration efficiency β on the force of adhesion F_{adh} for the monolithic filter. The particles are of equal size. (R denotes the number of experimental series)

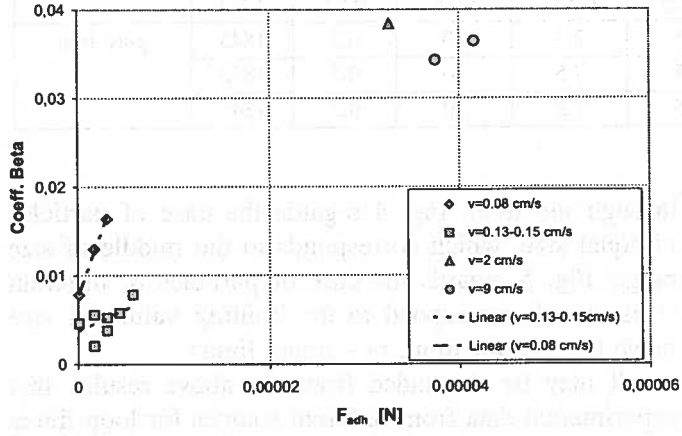

Fig. 5. Dependence of the coefficient of filtration efficiency β on the force of adhesion F_{adh} for the geometry of monolithic filter. The particles are of different sizes: r_1 – lower limit of experimental range, r_2 – upper limit. v denotes the velocity of metal flow

$\beta = 0.085 + 5137 \cdot F_{adh}$ with correlation coefficient $R^2 = 0.57$

• For monolithic filters and the particles of equal sizes, the flow velocity $v = 0.08$ cm/s (Fig. 4):

$\beta = 0.006 + 3422 \cdot F_{adh}$ with correlation coefficient $R^2 = 0.98$.

• For monolithic filters and the particles of different sizes, the flow velocity $v = 0.08$ cm/s (Fig. 5):

$\beta = 0.0077 + 2942 \cdot F_{adh}$ with correlation coefficient $R^2 = 0.99$.

• For monolithic filters and the particles of equal sizes, the flow velocity = 0.13 - 0.15 cm/s (Fig. 5):

$\beta = 0.0037 + 513 \cdot F_{adh}$ with correlation coefficient $R^2 = 0.37$.

The above relations are only approximate due to the insufficient experimental data. It results from the above considerations that the adhesion force is strongly dependent on the dimensions of interacting particles. Thus the desirable experimental data should be obtained for the uniform dimensions of inclusions, what is hardly possible even in laboratory conditions.

The comparison of results obtained for both types of filters reveals, that the coefficient β is an order of magnitude higher for loop filters. It results from different conditions of steel flow. In loop filters the metal flows perpendicularly to the loop planes. In monolithic filters the conditions for particles catch are less favorable, because the flow direction is generally parallel to the internal filter surface. The results for diverse steel flow velocities (Fig. 5) show, that in the case of monolithic filters the increase of the flow velocity has negative influence on the collision efficiency coefficient, and, consequently, on filtration efficiency.

It should be pointed out, that the relations for filtration efficiency for loop filters (5) and monolithic filters (7) deduced in the present work are simplified. They do not take into account the velocity of the metal flow through the filter, though the results of experiment [3–6] revealed, that the flow velocity influences filtration efficiency. Controversial opinions may be found in the literature, regarding the monolithic filters. Majority of authors: Ali *et al.* [4], Apelian *et al.* [5] and Raiber *et al.* [3] observed the decrease of filtration efficiency with the increase of flow velocity. The opposite was observed by Ichihashi *et al.* [6]. Their results refer to filters of very small channels and to flow velocities one or two orders of magnitude higher in comparison to other experiments. Unfortunately, the experimental data do not give the reliable dependence between the efficiency and the flow velocity for loop filters, because they greatly vary with loop sizes.

Another important factor influencing the filtration efficiency is the filter length. Relations (5) and (7) contain the filter length, while the experimental results [1, 4, 6] show only weak dependence of the filtration efficiency on this parameter. Ichihashi *et al.* [6] states the lack of dependence between filtration efficiency and the

filter length. In conditions of their experiment the drag force, proportional to the square of metal flow velocity, is so large that virtually no particles can be caught inside the filter. At moderate flow velocities filters of bigger length catch more tiny inclusions, and it only weakly influences the total oxygen content in steel, which is the measure of filtration efficiency. The prevailing part of bigger inclusions is captured at the filter entry, and the filtering efficiency in the end region of filter is low due to low amount of inclusions available, absence of metal stirring and slow diffusion. For this reason short filters of the length 2–4 cm are usually employed.

5. Relation between the force of adhesion and the neck radius

The force of inclusion adhesion is dependent on the size of the neck, which joins two inclusions. The reliability of the calculation of neck radius R_2 is thus decisive factor for correct value of F_{adh}. It results from the correctness of the model itself and from the radii of adhering particles. In Fig. 6 the values of neck radii

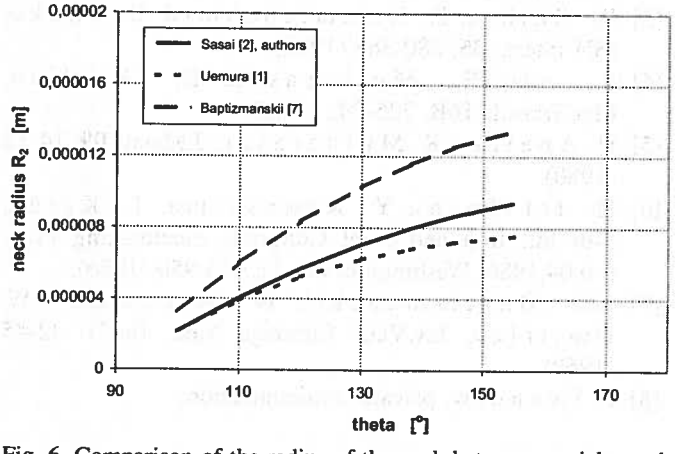

Fig. 6. Comparison of the radius of the neck between particles, calculated in the present work and in the publications [1, 2, 8]

calculated according to dependences given by various authors have been compared. The model equation obtained in the present work reduces to the dependence of Sasai *et al.* [2] for the case of inclusions of equal sizes. The model equation of Uemura *et al.* [1] differs from model equation (8) both for equal and different particles sizes. The numerical values calculated by Uemura *et al.* [1] are slightly lower. Baptizmanskii *et al.* [7] considered the model of adhesion of spherical particles of equal sizes. They calculated the neck radii from the change of surface energy due to the formation of new inter-phase surfaces (metal-gas and inclusion-gas) and to the reduction of the inter-phase surface metal-inclusion. The values of neck radius R_2 obtained from this model are about two times bigger in comparison to the results of other authors.

The experimental data of filtration efficiency were obtained for the population of particles of various dimensions, while calculations of adhesion force require the specified values of inclusions radii. The choice of these radii determines the values of the neck radius and the force of adhesion. In the present work four variants of particle sizes combinations were considered: particles of equal radii, which were in turn equal to the upper, middle and lower values of experimental range, and finally the particles of different radii, which were equal to upper and lower values of experimental range. In the Fig. 7 the results of calculations for the above mentioned variants and for three size ranges: $1{\cdot}10^{-6} - 2{\cdot}10^{-6}$, $1{\cdot}10^{-6} - 5{\cdot}10^{-6}$ and $5{\cdot}10^{-6}$ - 10^{-5} m are presented. For all size ranges the shape of dependence is the same. The values of adhesion force in the case of equal inclusions sizes are approximately two times higher for bigger particles (upper limit of size range) in comparison to smaller ones (lower limit). The other two variants show similar values of adhesion force, lying between the above extremes. These two last variants were taken for farther calculations.

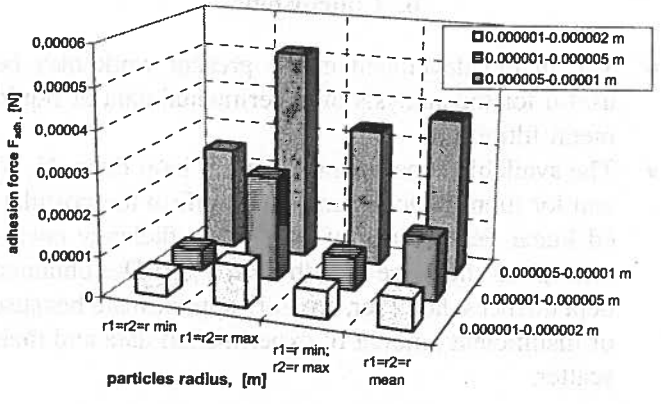

Fig. 7. Influence of the choice of particles radii for the calculated value of adhesion force for two classes of particles: a) $1{\cdot}10^{-6} - 2{\cdot}10^{-6}$, b) $1{\cdot}10^{-6} - 5{\cdot}10^{-6}$, and c) $5{\cdot}10^{-6}$ - 10^{-5} m

The influence of the size of the second particle on the neck radius, and the value of the adhesion force were also considered. This dependence is presented in Fig. 8. The initial values of the curves for neck radius R_2 ($1.1{\cdot}10^{-6}$ m) and for adhesion force F_{adh} ($1.26{\cdot}10^{-5}$ N) in the diagram correspond to the case of particles of equal radii ($r_1 = r_2 = 2.5{\cdot}10^{-6}$ m). With growing radius of the second particle the neck radius strongly increases and, at $r_2 > 5{\cdot}10^{-5}$ m, it reaches the constant value of $2{\cdot}10^{-6}$ m, i.e. 4/5 of the radius of smaller particle. Constant value of neck radius corresponds to the constant value of the force of adhesion $2.37{\cdot}10^{-5}$ N. This value is approximately two times higher, than in the case of equal

particles. This means, that the inclusion is more strongly attracted by the filter wall (the grains of filter material are much larger than the inclusions) than by the inclusions already attached. As it was mentioned earlier, the majority of particles sticks to these already attached to the walls. From this view-point the selection of particles radii used in calculations seems correct.

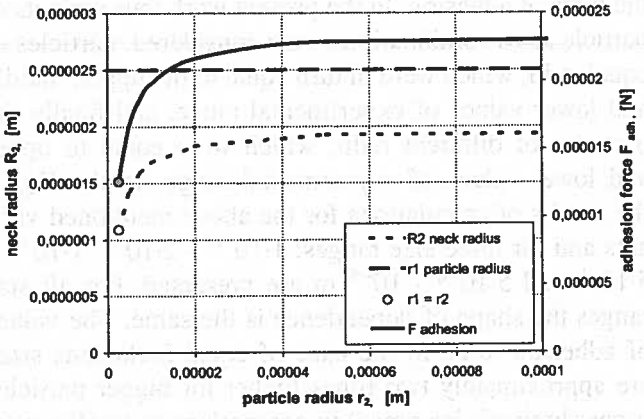

Fig. 8. Influence of the size of second particle on the calculated radius of the neck and adhesion force for the inclusion of the radius $r_1 = 2.5 \cdot 10^{-6}$ m

6. Conclusions

- The model developed in the present work may be useful for the analysis of experimental data of liquid metal filtration.
- The available experimental data for loop filters [1, 3] and for monolithic filters [3, 4] confirm the postulated linear dependence of collisions efficiency coefficient β on the force of adhesion F_{adh}. The obtained dependences, however, are only approximate because of insufficient amount of experimental data and their scatter.
- The proposed model allows for calculation of the radius of the neck, which forms between two particles due to withdrawal of the metal in the case of poor wetting between metal and particles.
- The known neck radius allows for calculation of the adhesion force of inclusion to the filter wall or another inclusion, already attached to the filter. The calculations in the present work reveal, that the adhesion to the filter wall is stronger than adhesion to another inclusion.

Received: 10 November 2005.

Acknowledgements

This work was financed by the Ministry of Education and Science – Project No 3T08B 011 26.

REFERENCES

[1] K. Uemura, M. Takahashi, S. Koyama, M. Nitta, ISIJ Intern. **32**, 150-6 (1992).
[2] K. Sasai, Y. Mizukami, ISIJ Internat. **41**, 1331-1339 (2001).
[3] K. Raiber, P. Hammerschmid, D. Janke, ISIJ Intern. **35**, 380-388 (1995).
[4] S. Ali, R. Mutharasan, D. Apelian, Met.Trans.B **16B**, 725-742 (1985).
[5] D. Apelian, R. Mutharasan, J.Metals **09**, 14-18 (1980).
[6] H. Ichihashi, Y. Kawashima, T. Kieda, 5-th Int. Iron and Steel Congress, Steelmaking Proc. 6-9.04.1986, Washington, **69** (1), 943-950 (1986).
[7] W.I. Baptizmanskii, N. Bachman, J.W. Dmitriev, Izv.VUZ Chernaja Met., (no3), 42-45 (1969).
[8] J. Iwanciw, private communication.